

## Hall effect enhanced low-field sensitivity in a three-contact extraordinary magnetoresistance sensor

Jian Sun and Jürgen Kosel

Citation: [Applied Physics Letters](#) **100**, 232407 (2012); doi: 10.1063/1.4726431

View online: <http://dx.doi.org/10.1063/1.4726431>

View Table of Contents: <http://scitation.aip.org/content/aip/journal/apl/100/23?ver=pdfcov>

Published by the [AIP Publishing](#)

---

### Articles you may be interested in

[Monitoring magnetization reversal and perpendicular anisotropy by the extraordinary Hall effect and anisotropic magnetoresistance.](#)

J. Appl. Phys. **108**, 043924 (2010); 10.1063/1.3475690

[Optimization of planar Hall resistance using biaxial currents in a NiO/NiFe bilayer: Enhancement of magnetic field sensitivity](#)

J. Appl. Phys. **88**, 3490 (2000); 10.1063/1.1289077

[Anisotropic low-field magnetoresistance of polycrystalline manganite sensors](#)

Appl. Phys. Lett. **74**, 2513 (1999); 10.1063/1.123024

[Low temperature thermometry in high magnetic fields. VII. Cernox™ sensors to 32 T](#)

Rev. Sci. Instrum. **70**, 104 (1999); 10.1063/1.1149549

[Low-field magnetoresistance in magnetic tunnel junctions prepared by contact masks and lithography: 25% magnetoresistance at 295 K in mega-ohm micron-sized junctions \(abstract\)](#)

J. Appl. Phys. **81**, 5521 (1997); 10.1063/1.364588

---

The advertisement features a dark blue background with white and yellow text. On the left, there is an image of a mobile phone and a desktop computer. In the center, there is an image of an Atomic Force Microscope (AFM). On the right, there is a large white text box containing promotional information. The Oxford Instruments logo is in the bottom right corner.

You don't still use this cell phone

or this computer

Why are you still using an AFM designed in the 80's?

**It is time to upgrade your AFM**

Minimum \$20,000 trade-in discount for purchases before August 31st

Asylum Research is today's technology leader in AFM

[dropmyoldAFM@oxinst.com](mailto:dropmyoldAFM@oxinst.com)

**OXFORD INSTRUMENTS**  
The Business of Science®

# Hall effect enhanced low-field sensitivity in a three-contact extraordinary magnetoresistance sensor

Jian Sun<sup>a)</sup> and Jürgen Kosel

Physical Sciences and Engineering Division, King Abdullah University of Science and Technology, Thuwal 23955-6900, Saudi Arabia

(Received 13 March 2012; accepted 21 May 2012; published online 6 June 2012)

An extraordinary magnetoresistance (EMR) device with a 3-contact geometry has been fabricated and characterized. A large enhancement of the output sensitivity at low magnetic fields compared to the conventional EMR device has been found, which can be attributed to an additional influence coming from the Hall effect. Output sensitivities of 0.19 mV/T at zero-field and 0.2 mV/T at 0.01 T have been measured in the device, which is equivalent to the ones of the conventional EMR sensors with a bias of  $\sim 0.04$  T. The exceptional performance of EMR sensors in the high field region is maintained in the 3-contact device. © 2012 American Institute of Physics. [<http://dx.doi.org/10.1063/1.4726431>]

It has been demonstrated that a strong magnetoresistance effect, the so-called extraordinary magnetoresistance (EMR), exists at room temperature in a certain kind of semiconductor/metal hybrid structure.<sup>1</sup> The orbital motion of carriers in a perpendicularly applied external field causes a current deflection resulting in a redistribution of the current from the metal shunt into the semiconductor layer, which is the main reason for the resistance increase. The fundamental principle of EMR is the change of the current path in the hybrid structure upon application of a magnetic field rather than the change of magnetoconductivity  $\sigma$  of either the semiconductor or the metal.<sup>2,3</sup> This effect is utilized to implement sensors for the measurement of magnetic fields perpendicular to the device.<sup>4-6</sup>

Experiments on the EMR effect were initially performed in a macroscopic composite Van der Pauw disk made of a semiconductor disk with a concentric metallic circular inhomogeneity embedded, and four electrodes were used to apply current and measure voltage (Fig. 1(a)).<sup>1</sup> Although this structure provided good results, its realization in mesoscopic and microscopic length scales is very difficult. Using bilinear transformation, a bar-type geometry, which is a semiconductor bar shunted by a metal stack on one side, has been derived from the Van der Pauw disk, showing a similar EMR effect and being simpler in terms of fabrication.<sup>7</sup> The EMR effect strongly depends on the geometry of the device and the placements of the electrical contacts. With respect to the placements of the electrodes, two major kinds of configurations can be distinguished: symmetric and asymmetric (Figs. 1(b) and 1(c)), where the placements of electrodes are symmetric to the central axis of the bar-type device or asymmetric, respectively.<sup>8</sup>

At high fields of  $\sim 0.1$  T, an outstanding sensitivity can be easily achieved with the symmetric EMR devices made of III-V materials. A two-contact EMR device has been reported recently exhibiting a strong sensitivity of 85  $\Omega$ /T at 0.1 T, which is comparable to that of GMR sensors used in recording applications.<sup>9</sup> Since the symmetric EMR device

has a parabolic magnetoresistance curve, it suffers from a weak low-field sensitivity limiting the applicability of EMR devices and hindering commercialization. Therefore, developing devices with improved low-field sensitivity would be an important contribution to further the potential of this technology. It has been shown that slightly enhanced low-field sensitivity can be obtained with an asymmetric electrode arrangement.<sup>10,11</sup> In this work, we describe a device with a 3-contact configuration, which combines the EMR effect and the Hall effect. The Hall effect has a linear response to a magnetic field change producing a considerable sensitivity in the low-field region. Due to this, the 3-contact device exhibits a significantly enhanced low-field sensitivity.

The semiconductor sample used in this work was deposited by solid-source molecular beam epitaxy on a semi-insulating GaAs substrate with the following structure: Substrate/ $\text{In}_x\text{Ga}_{1-x}\text{As}$  metamorphic buffer (1  $\mu\text{m}$ )/InAs stabilizing buffer (0.2  $\mu\text{m}$ )/Si-doped InAs active layer (1.5  $\mu\text{m}$ ,  $n = 10^{16} \text{ cm}^{-3}$ ). The metamorphic buffer was inserted between GaAs and InAs to accommodate the large lattice mismatch between them. A moderate mobility  $\mu$  of

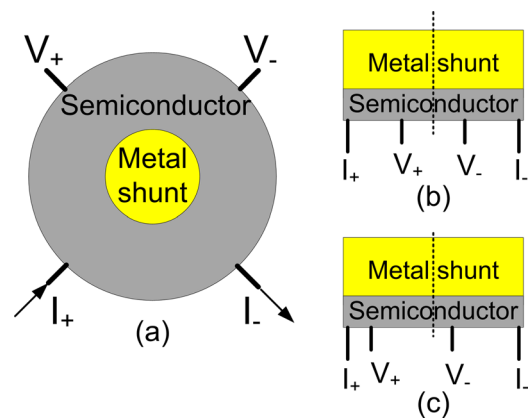


FIG. 1. Sketches of the conventional 4-contact EMR devices with (a) Van der Pauw disc geometry; (b) symmetric bar geometry; (c) asymmetric bar geometry. The dark lines labeled with  $I_+$ ,  $I_-$ ,  $V_+$ , and  $V_-$  represent the two current electrodes and two voltage probes, respectively. The dashed lines show the central axes of the bar-type devices.

<sup>a)</sup>Electronic mail: jian.sun@kaust.edu.sa.

$0.816 \text{ m}^2/\text{V}\cdot\text{s}$  and carrier density  $n_s$  of  $5.6 \times 10^{16} \text{ cm}^{-3}$  at 300 K has been observed in an unpatterned sample with the standard van der Pauw technique.

After growth, the semiconductor has been patterned into a rectangular mesa by photolithography followed by wet etching in citric acid solution exploiting the semi-insulating GaAs as an etch stop. The metal shunt and electrodes were metallized with a Ti (10 nm)/Au (150 nm) stack by magnetron sputtering. A low contact resistivity of  $\sim 10^{-7} \Omega \text{ cm}^2$  was realized after a rapid thermal annealing process at 250 °C. Fig. 2 shows the optical microscope image of a fabricated device. The current electrodes 1 and 2 were symmetrically placed at the two ends of the semiconductor bar with a separation of 50  $\mu\text{m}$  from the central line. At the central line, the voltage electrode 3 was connected to the metal shunt while electrode 4 was connected to the semiconductor bar. The output signal was measured through electrode 3 and 2. Electrode 4 was added to the device only to measure the reference signals for the sake of comparison. The distances between each electrode on the semiconductor bar and the edge of the metal shunt were 10  $\mu\text{m}$ .

The devices were wire bonded to a printed circuit board. The measurements and characterizations were carried out using a physical property measurement system. A homogeneous external field  $B$  ranging from  $-1$  to 1 T was applied in perpendicular direction to the devices in steps of 0.01 T. A constant current of 100  $\mu\text{A}$  was applied to the device via electrodes 1 and 2 throughout the measurements. The current transport in the hybrid structure is governed by Ohm's Law  $j = \sigma \cdot E$ , where  $E$  is the electric field and  $\sigma$  is the conductivity matrix, which is expressed as

$$\sigma = \frac{\sigma_0}{1 + \beta^2} \begin{bmatrix} 1 & -\beta \\ \beta & 1 \end{bmatrix},$$

where  $\beta = \mu H$  and  $\sigma_0 = \mu n e$  is the Drude conductivity without magnetic field,  $\mu$  is the mobility of the carriers,  $n$  is the carrier density, and  $e$  is the electric charge. With a high mobility semiconductor sample, a strong EMR effect can be expected. In steady state, the electrostatic potential  $\varphi(x, y)$  is described by  $\nabla \cdot [\sigma \cdot \nabla \varphi(x, y)] = 0$ . The output sensitivity  $\delta$  is defined as the rate of change of the output voltage  $V = \varphi(i) - \varphi(j)$ , where  $\varphi(i)$  and  $\varphi(j)$  are the potentials at electrode  $i$  and  $j$ , respectively, with respect to the magnetic field. The output voltage of the device can be expressed as

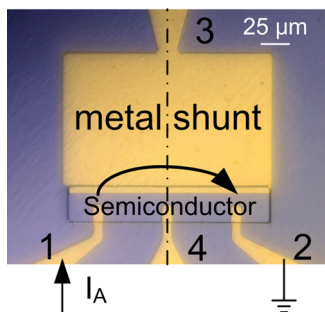


FIG. 2. Optical micrograph of the EMR device. The current is injected through the electrodes labeled as 1 and 2, and the arrow shows the direction of current flow. The output signal is measured through electrode 3 and 2. The external magnetic field is applied perpendicularly to the illustration plane.

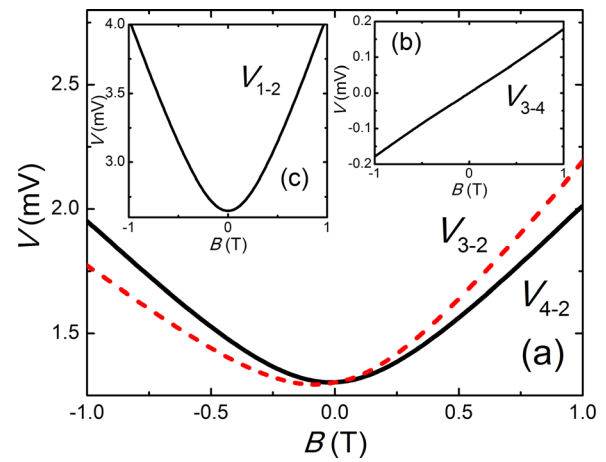


FIG. 3. Voltages between different electrodes as a function of the homogeneous magnetic field applied in perpendicular direction to the device.

$V_{3-2} = V_{3-4} + V_{4-2}$ , where  $V_{3-4}$  is the Hall voltage of the hybrid structure and  $V_{4-2}$  is the voltage arising from the asymmetric magnetoresistance  $R_{4-2}$ . The sensitivity of the device is calculated as  $\delta_{3-2} = \partial V_{3-2} / \partial B = \delta_{3-4} + \delta_{4-2}$ . Thus, in addition to a component  $\delta_{4-2}$  resulting from the asymmetric EMR effect of common sensors, the output sensitivity of this device is enhanced by a component  $\delta_{3-4}$ , which is caused by the Hall effect.

The voltages  $V_{i-j}$  measured between different electrodes are shown as a function of the magnetic field  $B$  in Fig. 3. The symmetric EMR voltage  $V_{1-2}$  of  $R_{1-2}$  was also measured for comparison. In the magnetic field range of  $\pm 0.25$  T, the output of the symmetric EMR  $V_{1-2}$  is approximately parabolic while the Hall voltage  $V_{3-4}$  has a linear behavior. Asymmetric  $V$  vs.  $B$  curves were observed for both asymmetric EMR voltages  $V_{4-2}$  and  $V_{3-2}$ , which represents the output of the 3-contact geometry. The difference between them,  $V_{3-2} - V_{4-2}$ , is equivalent to the Hall voltage  $V_{3-4}$ , as expected.

The sensitivities as a function of the magnetic field are shown in Fig. 4. The linear Hall response has a constant sensitivity  $\delta_{3-4}$  of  $\sim 0.16 \text{ mV/T}$ , while the outputs of the EMR effect become more sensitive as the field gets stronger. The

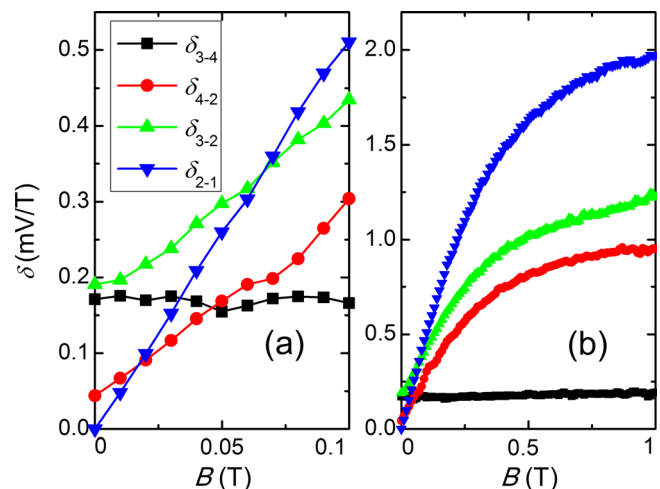


FIG. 4. Sensitivity versus magnetic field at (a) low-field region and (b) high-field region in the devices with different electrode configurations. Notice that the x-axes in (a) and (b) have different scales.

asymmetric EMR sensitivity  $\delta_{4-2}$  is slightly increased compared to the symmetric one  $\delta_{1-2}$  in the range of 0-0.015 T. The highest sensitivity at zero field is obtained between electrodes 3 and 2 with  $\delta_{3-2} = 0.19$  mV/T, which is equivalent to the one of the symmetric EMR  $\delta_{1-2}$  with a bias of 0.037 T and to the one of the asymmetric EMR  $\delta_{4-2}$  at 0.061 T. At  $B = 0.01$  T, which is a typical working range for low field applications like magnetic beads detection,  $\delta_{3-2}$  is as high as 0.2 mV/T compared to  $\delta_{4-2} = 0.067$  mV/T and  $\delta_{1-2} = 0.048$  mV/T. At the very high field regime, the device is still extremely sensitive though its performance is not quite as good as the one of a symmetric EMR device.

In conclusion, an EMR device with a 3-contact geometry, which combines the Hall effect and EMR effect, has been fabricated and characterized. The device shows a significant enhancement of the low-field output sensitivity. A value of 0.2 mV/T at 0.01 T has been measured, which is 5 times larger than that in a conventional symmetric EMR device. In order to achieve a similar sensitivity, the conventional EMR device needs an external bias field of at least 0.03 T. An even higher value can be expected in a device made of a semiconductor epilayer with higher mobility and with an optimized geometry that takes into account the EMR and Hall effect. These results extend the applicability of the EMR device into the low field region while maintaining an exceptional performance in the high field region. In our future work, we will study the performance of this device in the nano-scale regime to obtain a high spatial resolution, which is of interest for applications like reading heads. How-

ever, as the device size decreased to a value smaller than the mean free path, ballistic transport phenomena become to be more relevant having an impact on the device performance. It has been shown that the EMR effect still persists in such a case,<sup>12</sup> albeit the EMR ratio is expected to be smaller than in case of the diffusive transport regime.<sup>6</sup>

The authors wish to thank the staffs and facilities of the KAUST Advanced Nanofabrication, Imaging and Characterization Core Laboratory. The authors also would like to thank Bei Zhang for his help with PPMS measurements.

- <sup>1</sup>S. A. Solin, T. Thio, D. R. Hines, and J. J. Heremans, *Science* **289**, 1530 (2000).
- <sup>2</sup>J. Moussa, L. R. Ram-Mohan, J. Sullivan, T. Zhou, D. R. Hines, and S. A. Solin, *Phys. Rev. B* **64**, 184410 (2001).
- <sup>3</sup>A. C. H. Rowe and S. A. Solin, *Phys. Rev. B* **71**, 235323 (2005).
- <sup>4</sup>C. H. Moller, O. Kronenwerth, C. Heyn, and D. Grundler, *Appl. Phys. Lett.* **84**, 3343 (2004).
- <sup>5</sup>J. Moussa, L. Ram-Mohan, A. Rowe, and S. A. Solin, *J. Appl. Phys.* **94**, 1110 (2003).
- <sup>6</sup>S. A. Solin, D. R. Hines, A. Rowe, J. Tsai, and Y. Pashkin, *J. Vac. Sci. Technol. B* **21**, 3002 (2003).
- <sup>7</sup>T. Zhou, D. R. Hines, and S. A. Solin, *Appl. Phys. Lett.* **78**, 667 (2001).
- <sup>8</sup>J. Sun and J. Kosel, *IEEE Sens. J.* **12**, 1356 (2012).
- <sup>9</sup>J. Sun, S. B. Patil, Y.-A. Soh, and J. Kosel, *Appl. Phys. Express* **5**, 033002 (2012).
- <sup>10</sup>M. Holz, O. Kronenwerth, and D. Grundler, *Appl. Phys. Lett.* **86**, 172513 (2005).
- <sup>11</sup>T. D. Boone, N. Smith, L. Folks, J. A. Katine, E. E. Marinero, and B. A. Gurney, *IEEE Electron Device Lett.* **30**, 117 (2009).
- <sup>12</sup>T. D. Boone, L. Folks, J. A. Katine, S. Maat, E. Marinero, S. Nicoletti, M. Field, G. J. Sullivan, A. Ikhlassi, B. Brar, and B. A. Gurney, *IEEE Trans. Mag.* **42**, 3270 (2006).